Chiral Nematic Hydrogels

DOI: 10.1002/anie.201302687

Responsive Photonic Hydrogels Based on Nanocrystalline Cellulose**

*Joel A. Kelly, Amber M. Shukaliak, Clement C. Y. Cheung, Kevin E. Shopsowitz, Wadood Y. Hamad, and Mark J. MacLachlan**

Stimuli-responsive photonic materials are useful in sensors, optical filters, inks, displays, and other technologies.[1,2] In particular, photonic hydrogels can show large color changes in response to variations in osmotic pressure, and have a wide range of tunable functionality through selection of suitable hydrogel monomer(s).[3–5] Chiral nematic liquid crystals (LCs) can have unique photonic properties that could be valuable in the form of a hydrogel.[6] Although there are some reports of photonic hydrogels with chiral nematic structures prepared mostly through polymerization of functionalized molecular LCs,[7] a general approach to achieve the broad range of responsive functionalities found in conventional hydrogels (for example, temperature, pH, solvent) is still lacking. Herein we report novel nanocomposite hydrogels prepared by self-assembly of nanocrystalline cellulose (NCC) with various hydrogel monomers. These new chiral nematic hydrogels have tunable colors, respond to various stimuli, and have interesting mechanical and swelling behavior. We demonstrate that the hydrogels can be prepared as large, freestanding films and can be photopatterned. Furthermore, the embedded NCC offers new potential for modification to produce functional materials. Our findings will be important for developing sensors and other chiral optoelectronic devices.

Materials with chiral nematic order show selective reflection of light with circular polarization. They currently have applications such as distributed feedback lasing and polarized photoluminescence.[6] To construct a photonic hydrogel with chiral nematic order, we turned to cellulose, a widely-available, inexpensive, and biocompatible material. Cellulose-based hydrogels are used commercially in wound dressings, superabsorbent materials, and other applications.[8] The surface of cellulose and its derivatives can be tailored to produce hydrogels that respond to external stimuli such as temperature or pH.[9]

Nanocrystalline cellulose (NCC), prepared by acid hydrolysis of cellulose,[10–12] has been used to reinforce hydrogels to improve their typically poor mechanical properties.[13–16] NCC forms a chiral nematic LC phase in water, where the NCC rods are organized in a left-handed helical assembly. These lyotropic phases exhibit photonic color when the helical pitch of the assembly is on the order of the wavelength of visible light, selectively reflecting left-handed circularly polarized light. Tatsumi et al. recently created a hydrogel with liquid crystalline order using NCC, but it did not show any photonic properties.[15]

A main criterion to successfully prepare photonic hydrogels using NCC was to find suitable conditions for polymerization of hydrogel precursors while retaining the formation of the chiral nematic phase of NCC, which is very sensitive to changes in pH and ionic strength.[17] In our experiments, we used sulfuric acid hydrolysis to prepare acidic dispersions of NCC. Mixing NCC (3 wt%, pH 2.4) with nonionic hydrogel precursors (that is, monomer, cross-linker and photoinitiator) forms a chiral nematic phase upon evaporation-induced self assembly (EISA), as shown by polarized optical microscopy (POM). For example, POM of NCC and acrylamide (AAm) mixtures shows the emergence of spherulites during evaporation that is due to the formation of a chiral nematic phase, up to an AAm/NCC ratio of 2.7:1 by weight (Figure 1a). Similar results are observed for other hydrogel monomers and cross-linkers frequently used to prepare responsive hydrogels, such as N-isopropylacrylamide (NIPAm), acrylic acid (AAc), 2-hydroxyethylmethacrylate (HEMa) polyethylene glycol methacrylate (PEGMa), *N*,*N*′-methylenebisacrylamide (bis), and polyethylene glycol dimethacrylate (DiPEGMa). At any stage during EISA, polymerization may be initiated by UV irradiation to lock in place the self-assembled structure.

The precursor composition and evaporation time can be varied to access a wide range of nanocomposite hydrogels with chiral nematic organization (essentially, any NCC concentration greater than the threshold for full anisotropy, typically 10–12% in sulfated NCC aqueous dispersions).[18] Polymerizing a dispersion at low NCC concentration (for example, a final concentration of 10.5 wt% NCC, 17.4 wt% AAm and 0.34 wt% bis) yields a pliable, transparent film with regions exhibiting a fingerprint-like anisotropic texture observable by POM (Figure 1b). Nanocomposite hydrogels with iridescence, arising from a helical pitch on the order of the wavelengths of visible light, can be prepared at high NCC concentration and allowing the dispersion to evaporate to dryness before polymerization (for example, to a final composition of 64.4 wt% NCC, 33.5 wt% AAm and 2.1 wt% bis). Increasing the ionic strength of the dispersion by adding salts such as sodium chloride, which is known to decrease the helical pitch of NCC chiral nematic phases,[17] produces nanocomposite hydrogels with reflected color

[*] Dr. J. A. Kelly, A. M. Shukaliak, C. C. Y. Cheung, K. E. Shopsowitz, Prof. M. J. MacLachlan
Department of Chemistry, University of British Columbia
2036 Main Mall, Vancouver, BC, V6T 1Z1 (Canada)
E-mail: mmaclach@chem.ubc.ca
Dr. W. Y. Hamad
CelluForce, Inc.
3800 Wesbrook Mall, Vancouver, BC, V6S 2L9 (Canada)

[**] We thank CelluForce and NSERC for supporting this project. J.A.K. is grateful to NSERC for a Postdoctoral Fellowship.

Supporting information for this article is available on the WWW under http://dx.doi.org/10.1002/anie.201302687.

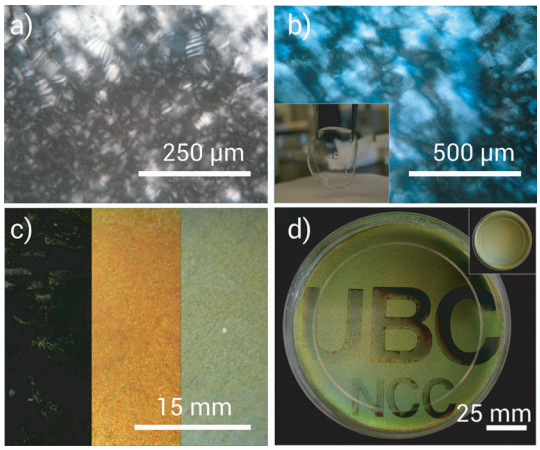

Figure 1. Formation of chiral nematic structure in nanocomposite hydrogels at varying composition. a) POM image of a NCC/acrylamide dispersion during evaporation showing the formation of spherulites characteristic of chiral nematic ordering. b) POM of a PAAm nanocomposite prepared with high acrylamide loading (10 wt% NCC) swollen in water, showing fingerprint texture locked in place by photopolymerization (inset: a photograph of the swollen transparent hydrogel). c) Photographs of iridescent PAAm nanocomposite hydrogels (66 wt% NCC) and varying amounts of sodium chloride; increasing the ionic strength blue-shifts the reflectance across the visible region (transmission spectra are given in the Supporting Information, Figure S1). d) Photograph of an iridescent photopatterned PAAm nanocomposite as the film swells in water. The masked region swells at a faster rate, producing a latent image (a photograph of the patterned film before swelling is given in in the inset).

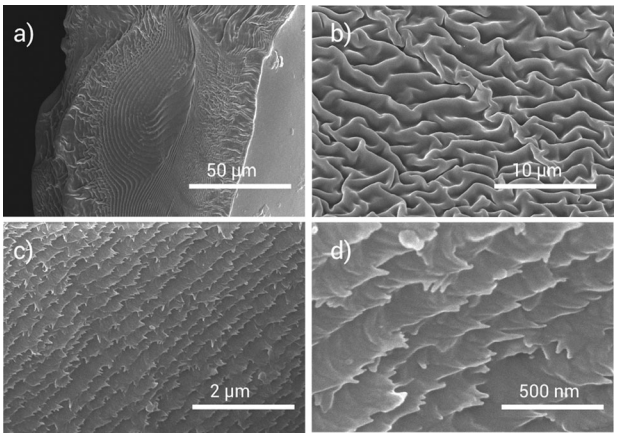

Figure 2. SEM images of PAAm nanocomposite prepared at varying NCC/AAm compositions. a) Top view of a PAAm nanocomposite with high AAm loading (10 wt% NCC) shows a smooth surface and a layered structure with a fingerprint defect present. b) Higher magnification reveals a wrinkled texture and a helical pitch distance of several micrometers. c) Side view of an iridescent PAAm nanocomposite (66 wt% NCC) shows a helical pitch distance of hundreds of nanometers. d) Higher magnification of the iridescent PAAm nanocomposite shows the left-handed rod morphology characteristic of NCC chiral nematic phases.

spanning the near-infrared and visible regions of the electromagnetic spectrum (Figure 1c; Supporting Information, Figure S1). The reflection bands are broad in comparison to molecular planar chiral nematic LCs; this is characteristic of dried NCC chiral nematic phases and likely originates from the polydispersity of the NCC mesogens and misalignment of the chiral nematic domains.

Scanning electron microscopy (SEM) of the dried nanocomposites reveals a layered structure and a smooth surface, consistent with the chiral nematic texture observed by POM. Hydrogels with low NCC content have a wrinkled structure with a repeat distance of several micrometers throughout the thickness of the film (Figure 2a,b). In comparison, SEM of an iridescent hydrogel with high NCC content showed a much shorter helical pitch, on the order of hundreds of nanometers in keeping with its iridescence (Figure 2c). At higher magnification, the left-handed twisting rod morphology of the NCC chiral nematic phase is evident, resembling micrographs of pure NCC (Figure 2d).[19]

The nanocomposite hydrogels respond to variations in swelling with a change in the helical pitch of the chiral nematic phase and a concomitant change in the iridescence. Immersing a blue iridescent PAAm sample in water causes an immediate red-shift as the film swells, reaching equilibrium in the near-IR after about 150 s (Figure 3a; Supporting Information, Figure S2). A POM video of this nanocomposite hydrogel during swelling shows strong birefringence that is retained as the color red-shifts, which is due to the intrinsic birefringence of NCC. The extent and rate of swelling is correlated with the polymerization time; increasing the UV irradiation time reduces the extent and rate of swelling (Supporting Information, Figure S3). It is interesting to note that films prepared in the dark remain intact during immersion in water, and swell very rapidly, red-shifting their iridescence into the near-IR. This can be exploited to produce a latent image that appears only when the film is immersed in water as the masked region rapidly swells (Figure 1d). This could enable application of the nanocomposite hydrogels as a security feature or patterned sensor.

Slow swelling kinetics and poor mechanical properties typical of photonic hydrogels can be regarded as major limitations to their deployment in many of their anticipated applications such as point-of-care optical sensors. In comparison to other photonic hydrogels, which can take up to several hours to equilibrate during swelling,[20] we suggest the fast swelling response of the NCC-based nanocomposites is related to their toughness and high Young's modulus, which has been shown to correlate with hydrogel network diffusion kinetics.[21] Improved mechanical performance of the iridescent nanocomposites stems from the formation of a percolated NCC network acting as a high-performance reinforcement (Supporting Information, Figure S4); it is also plausible that NCC effectively increases the cross-linking density of the hydrogel polymer.[15,16] Other stimuli-responsive NCC-reinforced polymer nanocomposites have also been shown to exhibit similar mechanical performance, and difference between dry and swollen states.[22]

The reflected color of the nanocomposite hydrogels can be reversibly controlled by swelling in various media. For example, a rapid blue-shift of a hydrated PAAm nanocomposite is observed upon immersion in pure ethanol (Figure 3b; Supporting Information, Figure S5), reaching equilibrium in about 150 s. Soaking a swollen PAAm nano-

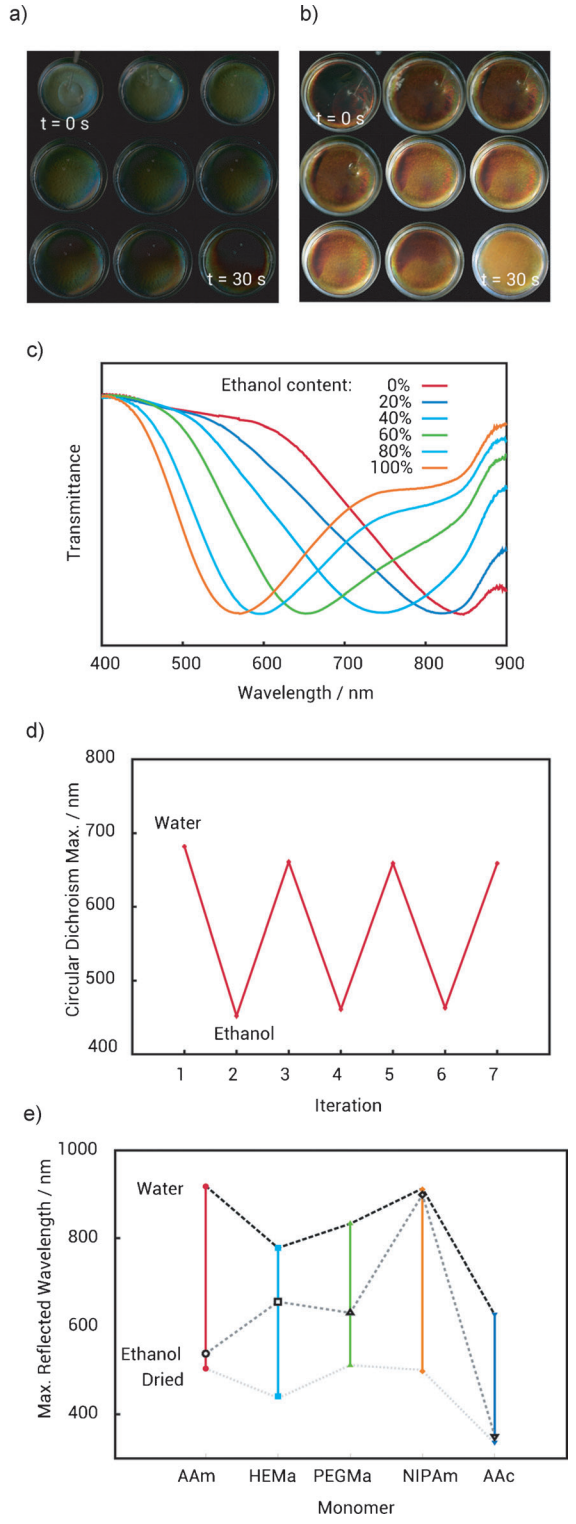

Figure 3. Swelling of the nanocomposite hydrogels (66 wt% NCC). Photographs of a 6 cm diameter PAAm hydrogel as it swells in water (a) and contracts in ethanol (b) (transmission spectra and kinetics measurements are given in the Supporting Information, Figures S2, S3, and S5). c) Transmission spectra of a PAAm nanocomposite in varying concentrations of aqueous ethanol. d) The change in maximum reflected wavelength measured by circular dichroism of a PAAm hydrogel soaked alternately in water and ethanol. e) The maximum reflected wavelength as a function of hydrogel monomer in dry, aqueous, and ethanolic states.

composite in water/ethanol mixtures causes a gradual blue-shift with increasing ethanol content (Figure 3c). Circular dichroism (CD) of the PAAm hydrogels soaked in water and ethanol showed a strong positive ellipticity that arises from the reflection of left-handed circularly polarized light from the chiral nematic phase (Supporting Information, Figure S6).

The color changes are fully reversible; the nanocomposite hydrogels could be immersed in various media, or dried and reswollen in water for multiple cycles with no apparent change in the chiral nematic optical properties (Figure 3d). The swelling response of the iridescent hydrogel nanocomposites can be tailored through selection of a suitable hydrogel monomer. For example, whereas PNIPAm and PAAm nanocomposites have similar near-IR iridescence after swelling in water, PNIPAm nanocomposites do not de-swell upon immersion in ethanol, retaining a maximum reflected wavelength of about 900 nm while PAAm nanocomposites de-swell to reflect at about 550 nm (Figure 3e). Nanocomposites made with PHEMa, a hydrogel polymer known to exhibit increased swelling in ethanol owing to favorable free energy of mixing,[23] instead show a blue-shift in their reflected color upon immersing a water-swollen nanocomposite in ethanol. Conversely, the swelling response in water from all nanocomposites is more stable towards changes in ionic strength (Supporting Information, Figure S7). Given the significant NCC loading of our hydrogels, we note the potential for strong hydrogen bonding interactions between NCC and hydrogel polymers and interactions within the percolated NCC network to likely contribute to the unique swelling behavior of these iridescent hydrogels.

Nanocomposite hydrogels with responsive functionality to various stimuli can be prepared through choice of suitable hydrogel monomer. For example, PAAc nanocomposites show a red-shift in their iridescence with increasing pH from pH 8–13 (Figure 4a). Again, swelling from a dry state is very rapid in comparison to the kinetics of conventional photonic hydrogels;[20,23] iridescence from nanocomposites immersed in aqueous solutions at pH 9.5 and pH 7 can be differentiated within about 200 s (Figure 4b). Similarly, heating an iridescent PNIPAm nanocomposite above the lower critical solution temperature of PNIPAm (ca. 31 °C for pure PNIPAm)[24] induced a reversible blue-shift of about 40 nm in the reflected wavelength, which is due to the transition of PNIPAm from a swollen hydrophilic to a shrunken hydrophobic state (Supporting Information, Figure S8).

We can also install responsive functionality in the nanocomposite hydrogels through NCC surface modification after hydrogel polymerization. As prepared, the NCC contains acidic sulfate ester surface groups (ca. 1 sulfate group per 20 anhydroglucose units[25]), which undergo cation exchange within the hydrogel nanocomposite upon neutralizing the gel in a dilute solution of base.[17] The PAAm nanocomposites exhibit increased swelling and red-shifted color in methanol, ethanol, or even acetone or isopropanol as the size and hydrophobicity of the cation increases (Figure 4c). We hypothesize that the change in swelling is likely due to the influence of the cation on hydrogen bonding interactions between NCC and PAAm, rather than degradation of the polymer or NCC, as Fourier transform-IR (FTIR) spectros-

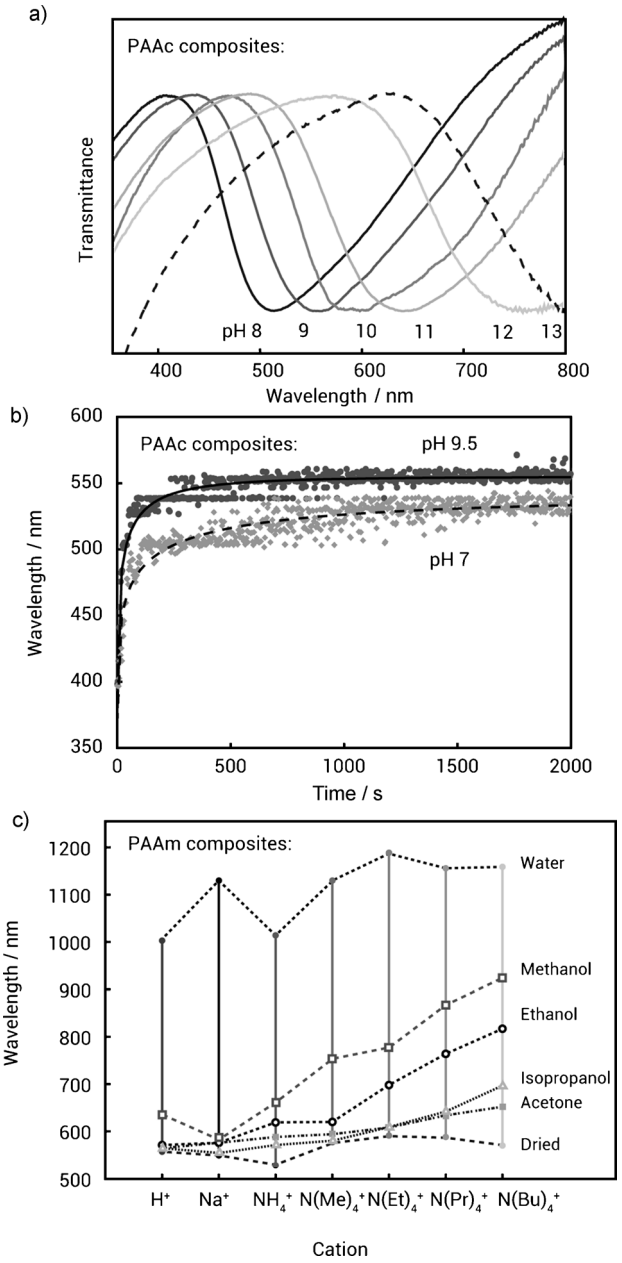

Figure 4. Responsive behavior from the nanocomposite hydrogels. a) Transmission spectra of a PAAc nanocomposite (50 wt% NCC) in different basic solutions showing a red-shift with increasing pH. b) Time dependence of the reflected color from a PAAc nanocomposite (66 wt% NCC) immersed in pH 7 and pH 9.5 aqueous solutions (lines drawn to guide the eye). c) The maximum reflected wavelength of a cation-exchanged PAAm/NCC nanocomposite as a function of cation for dry, aqueous, and organic-solvent-swollen states.

copy shows negligible change in the nanocomposite after modification (Supporting Information, Figure S9). We envision the ability to carry out NCC surface modification inside of a pre-assembled chiral nematic phase will also be useful to prepare new materials with chiral nematic properties whose precursors are incompatible with EISA.

In summary, our results demonstrate a straightforward and general method to prepare novel nanocomposite hydrogels that have long-range chiral nematic structure and photonic properties. The hydrogels show changes in iridescence in response to external stimuli such as solvent, pH, or temperature. Furthermore, NCC surface modification within the hydrogel holds promise as a new approach to tailoring the material's response, and to prepare new materials with chiral optoelectronic properties. We expect these nanocomposite materials will be useful in applications that exploit their photonic properties, such as sensors or tunable filters, and also as soft templates for new materials.

Experimental Section

Nanocrystalline cellulose (NCC) was prepared from sulfuric acid hydrolysis of bleached kraft softwood pulp as previously described.[26] Hydrogel nanocomposites with chiral nematic structure were prepared by mixing a 3 wt% aqueous NCC dispersion with hydrogel precursors (monomer, crosslinker, and 2,2-diethoxyacetophenone as photo-initiator), stirring for 1 h to ensure homogeneity, and casting the mixture in a polystyrene Petri dish to evaporate to a desired concentration. Photo-polymerization was carried out for 1 h using illumination from an 8 W 300 nm (UV-B) light source. A typical preparation for a hydrogel nanocomposite with a large chiral nematic pitch had a NCC/AAm/bis/initiator ratio of 0.6:1:0.02:0.03, and was polymerized at a final concentration of 10.5 wt% NCC by weighing the dispersion throughout EISA. A nanocomposite with near-IR iridescence could be prepared with a NCC/AAm/bis/photoinitiator ratio of 1:0.52:0.03:0.05 and allowing the mixture to evaporate to dryness before photo-polymerization (that is, 62 wt% NCC, 32% AAm, 2% bis and 3% initiator). Additional samples were prepared by adding small amounts of aqueous sodium chloride to the mixture before evaporation to blue-shift the chiral nematic photonic reflection. To carry out cation exchange on a PAAm/NCC hydrogel, the hydrogel was first soaked in water overnight and then immersed in a 0.01M aqueous solution of base (for example, NR_4OH, R = H, methyl, butyl, etc.) for 4 days. The reacted films were removed and soaked in water to remove excess base.

Static transmission UV/Vis/near-IR spectra were collected with a Cary 5000 UV/Vis/NIR spectrophotometer on samples mounted normal to the beam. The maximum reflected wavelength varied by about 30 nm in different regions of each sample. Timed transmission experiments were collected using an Ocean Optics spectrometer and a deuterium/halogen source. Polarized optical microscopy was performed using crossed polarizers on an Olympus BX41 microscope. SEM images were collected using a Hitachi S4700 electron microscope on samples sputter-coated with gold. Circular dichroism spectroscopy experiments were performed using a JASCO J-710 spectropolarimeter on samples mounted normal to the beam. Infrared spectra were obtained with a Nicolet 6700 FTIR equipped with a Smart Orbit diamond attenuated total reflectance (ATR) attachment. Tensile strength measurements were carried out on 15 mm × 5 mm strips at a rate of 0.1 mm min^{-1} using a Deben microtensile stage equipped with a 200 N load cell.

Received: April 1, 2013
Revised: May 24, 2013
Published online: July 23, 2013

Keywords: gels · liquid crystals · polymers · self-assembly · sensors

[1] C. I. Aguirre, E. Reguera, A. Stein, *Adv. Funct. Mater.* **2010**, *20*, 2565 – 2578.
[2] G. von Freymann, V. Kitaev, B. V. Lotsch, G. A. Ozin, *Chem. Soc. Rev.* **2013**, *42*, 2528 – 2554.

[3] S. Asher, J. Holtz, J. Weissman, G. Pan, *MRS Bull.* **1998**, *23*, 44 – 50.
[4] J. Ge, Y. Yin, *Angew. Chem.* **2011**, *123*, 1530 – 1561; *Angew. Chem. Int. Ed.* **2011**, *50*, 1492 – 1522.
[5] Z. L. Wu, J. P. Gong, *NPG Asia Mater.* **2011**, *3*, 57 – 64.
[6] M. O'Neill, S. M. Kelly, *Adv. Mater.* **2003**, *15*, 1135 – 1146.
[7] D. J. Broer, C. M. W. Bastiaansen, M. G. Debije, A. P. H. J. Schenning, *Angew. Chem.* **2012**, *124*, 7210 – 7218; *Angew. Chem. Int. Ed.* **2012**, *51*, 7102 – 7109.
[8] A. Sannino, C. Demitri, M. Madaghiele, *Materials* **2009**, *2*, 353 – 373.
[9] A. E. Way, L. Hsu, K. Shanmuganathan, C. Weder, S. J. Rowan, *ACS Macro Lett.* **2012**, *1*, 1001 – 1006.
[10] Y. Habibi, L. A. Lucia, O. J. Rojas, *Chem. Rev.* **2010**, *110*, 3479 – 3500.
[11] D. Klemm, F. Kramer, S. Moritz, T. Lindström, M. Ankerfors, D. Gray, A. Dorris, *Angew. Chem.* **2011**, *123*, 5550 – 5580; *Angew. Chem. Int. Ed.* **2011**, *50*, 5438 – 5466.
[12] B. L. Peng, N. Dhar, H. L. Liu, K. C. Tam, *Can. J. Chem. Eng.* **2011**, *89*, 1191 – 1206.
[13] S. Su, W. Y. Hamad, (FPInnovations), US Patent 2011/0182990, **2011**.
[14] T. Abitbol, T. Johnstone, T. M. Quinn, D. G. Gray, *Soft Matter* **2011**, *7*, 2373 – 2379.
[15] M. Tatsumi, Y. Teramoto, Y. Nishio, *Biomacromolecules* **2012**, *13*, 1584 – 1591.
[16] J. Yang, C. R. Han, J. F. Duan, M. G. Ma, X. M. Zhang, F. Xu, R. C. Sun, X. M. Xie, *J. Mater. Chem.* **2012**, *22*, 22467 – 22480.
[17] X. M. Dong, D. G. Gray, *Langmuir* **1997**, *13*, 2404 – 2409.
[18] E. E. Ureña-Benavides, G. Ao, V. A. Davis, C. L. Kitchens, *Macromolecules* **2011**, *44*, 8990 – 8998.
[19] J. Majoinen, E. Kontturi, O. Ikkala, D. G. Gray, *Cellulose* **2012**, *19*, 1599 – 1605.
[20] M. Ben-Moshe, V. L. Alexeev, S. A. Asher, *Anal. Chem.* **2006**, *78*, 5149 – 5157.
[21] T. Tanaka, D. J. Fillmore, *J. Chem. Phys.* **1979**, *70*, 1214 – 1218.
[22] J. R. Capadona, K. Shanmuganathan, D. J. Tyler, S. J. Rowan, C. Weder, *Science* **2008**, *319*, 1370 – 1374.
[23] X. Xu, A. V. Goponenko, S. A. Asher, *J. Am. Chem. Soc.* **2008**, *130*, 3113 – 3119.
[24] L. Hu, M. J. Serpe, *Polymers* **2012**, *4*, 134 – 149.
[25] W. Y. Hamad, T. Q. Hu, *Can. J. Chem. Eng.* **2010**, *88*, 392 – 402.
[26] K. E. Shopsowitz, W. Y. Hamad, M. J. MacLachlan, *J. Am. Chem. Soc.* **2012**, *134*, 867 – 870.

